CREATION OF A VIRTUAL AQUATIC MESOCOSM USING STELLA SOFTWARE

P. D. Schreuders, C. Nagoda, A. Lomander, G. Gipson, J. Rebar, X. Cheng

ABSTRACT. *This study creates both virtual and physical, closed, aquatic mesocosms. Each mesocosm consisted of a 10 gal aquarium with an unspecified proportion of water and air. The contents of the aquarium included several crayfish, dechlorinated water, gravel, and submerged aquatic and terrestrial plants. The mesocosm was self–sustaining, airtight, watertight, and food tight. By reaching equilibrium between primary production, waste production and degradation, food consumption, and respiration (consumed oxygen and produced carbon dioxide), it was possible to keep the physical system self–sustained for up to a month. Parameters obtained from the physical mesocosms describe how changes in some parameters affected others. The ecological considerations that were important for the modeling procedure dealt with the trophic levels (producer, consumer, or decomposer) of the individual organism communities and their relationships. We defined the equations and parameters that describe the transfers of mass and energy between the organisms and their physical environment. The virtual mesocosm was based on a series of models for growth, oxygen consumption, biodegradation, nitrogenous component degradation, photosynthesis, and respiration. Development of the Stella model was an iterative process; the results of successive simulations were compared with results from physical crayfish aquaria to calibrate the model for improved accuracy.*

Keywords. *Anacharis, Crayfish, Ecological model, Mesocosm, Simulation, Stella.*

The complex relationships in any ecosystem present a challenge to the researcher and an even more formidable challenge to the designer. Thus, modeling of an ecosystem via computer simulation has become a widely studied and important tool for understanding and predicting the behavior of complex systems (Beyers and Odum, 1993; Odum and Odum, 2000). In this article, we examine a simplified ecosystem, a mesocosm. Although more complex ecosystems have been successfully modeled (e.g., Parrott and Kok, 2001, 2002), our simplified system has its own unique benefits that make it a functional learning tool. While it is recognized that scaling issues and reductions in species diversity limit the direct applicability of microcosm– and mesocosm–based data to natural ecosystems (Kangas, 2004), this system is amenable to both physical and numerical modeling and was, therefore, an excellent prototype for teaching ecological engineering design. Ecological engineering has been defined as "the design of human society with its natural environment for the benefit of both" (Mitsch and Cronk, 1992). Furthermore, this pair of models (virtual and physical) provides a successful balance between the de-

tail found in models of more complex ecosystems and the clarity necessary to demonstrate causality in an introductory course. The mesocosms were used to teach ecological systems design to seniors enrolled in a biological engineering course (Schreuders et al., 2002).

The mesocosm consisted of a 10 gal fish tank containing gravel and water. Two to four crayfish were placed in the tank along with terrestrial and submerged aquatic plants. The system was then sealed for up to one month, after which the success of the design was evaluated. Multiple possible "steady–state" results could occur in the mesocosm. These ranged from survival of all the biota to death of the crayfish and plants. The small tank size and time constraints allowed only a limited possibility of self–organization to yield a successful result, particularly if the initial conditions were ill chosen. However, if the initial conditions were near the desired steady state, the mesocosm was more likely to organize towards that state (Mitsch and Wilson, 1996).

The virtual mesocosm was created to support physical mesocosm design by helping to avoid inappropriate initial conditions. The Stella software package (Stella, 1997) was used for the computer modeling and simulation. The simulation was developed from equations in the literature and phenomenological data from the physical mesocosms. By iteratively evaluating and refining the physical and virtual mesocosms, both models were strengthened.

ECOLOGICAL CONSIDERATIONS AND ASSUMPTIONS

The modeling of ecological systems focuses primarily on the flux of matter and energy through the various producer, consumer, and decomposer pathways composed of the individual organisms in the ecosystem. On a global scale,

The authors are **Paul D. Schreuders, ASAE Member Engineer,** Assistant Professor, Department of Engineering and Technology Education, Utah State University, Logan, Utah; **Carey M. Nagoda,** Graduate Student, **Andrea Lomander,** Graduate Student, **Joyce E. Rebar,** Graduate Student, and **Xuemei Cheng,** Graduate Student, Department of Biological Resources Engineering, University of Maryland, College Park, Maryland; and **Geoffrey T. Gipson,** Graduate Student, Program in Toxicology, University of Maryland, Baltimore, Maryland. **Corresponding author:** Paul D. Schreuders, Engineering and Technology Education, Utah State University, 6000 Old Main Hill, Logan, UT 84322; phone: 435–797–7559; fax: 435–797–2567; e–mail: pschreuders@cc.usu. edu.

these pathways are effectively closed, except entering solar energy that leaves the system via various mechanisms, and create the major material cycles involved in sustaining the global biosphere. In the process of constructing a smaller scale model of an ecosystem (whether physically in a tank or virtually on a computer), attention must be paid to the establishment of these cycles (particularly the oxygen, carbon, and nitrogen cycles) to sustain the various biota in the ecosystem. The ecological relationships between the organisms are a critical aspect of these cycles. Communities of organisms establish food webs, with the position of an organism in the web determining its trophic level. The major trophic levels in an ecosystem include the primary producers, primary consumers, and decomposers. All trophic communities must be functioning properly for the establishment of the requisite material cycles. For this reason, representative organisms from each of the aforementioned trophic levels were included in the model. In addition to direct mass and information linkages, the three trophic levels were linked through the dynamics of the carbon, oxygen, and nitrogen cycles (fig. 1).

PRIMARY PRODUCERS: THE PLANTS

The organic matter that supports all biological activity in freshwater ecosystems is manufactured through the photosynthesis of phytoplankton (algae) and higher plants, typically called the *producers* or *autotrophs* of an ecosystem. Primary production is the process by which inorganic carbon (usually in the form of carbon dioxide) is fixed into organic forms in biomass, producing oxygen, which other organisms use for respiration. The energy and matter fixed in this biomass are then transferred to various levels within the ecosystem (Adey and Loveland, 1998). The transfer routes are initiated by herbivores that graze on the algal and plant cell biomass or by detritivores and microbes that consume waste organic matter after the senescence and death of the producer (Valiela, 1991).

The plants included in the physical mesocosm (and modeled in the virtual mesocosm) were a submerged aquatic (anacharis) and a terrestrial legume (alfalfa). Anacharis (*Elodea canadensis*) is a freshwater submerged macrophyte commonly included in aquaria for its fast growth, oxygen production and carbon sequestering, and nutrient uptake capabilities. Alfalfa (*Medicago sativa*) was grown at the interface between water and enclosed gases. This species is capable of symbiotic nitrogen fixation with appropriate root
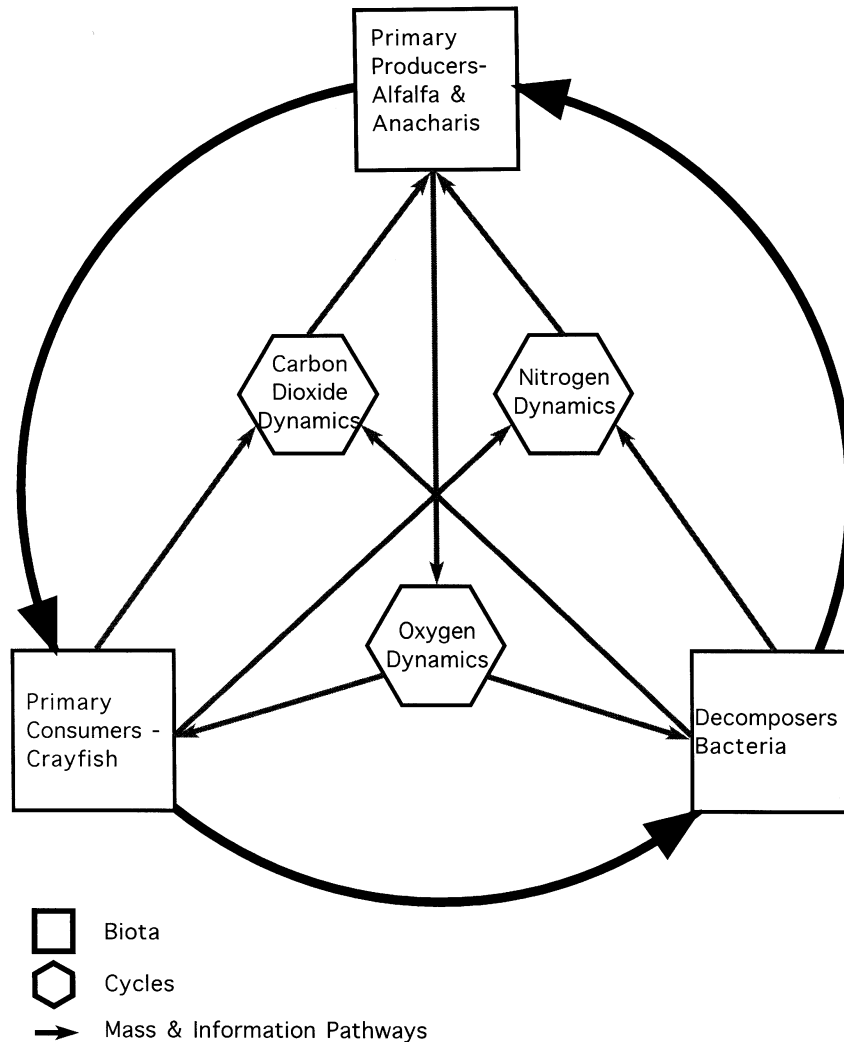

Figure 1. Schematic of the model structure showing the six primary elements and the mass and information flows between them (Schreuders et al., 2002).

nodule bacteria and allowed for photosynthetic oxygen production in the sealed tank's headspace. Algal growth on gravel and tank walls was not taken into consideration in the model development, but was instead merged into the growth of the anacharis.

Net primary production in an ecosystem (the gross total photosynthesis minus the respiration of the producer organisms) may be controlled by a number of external factors, primarily temperature, light, and nutrient concentrations (Valiela, 1991). Temperature was a major external forcing function on all biological processes and affected the overall rate of photosynthesis. Experience with the physical model confirmed that light was the other major external forcing function on photosynthesis. The amount of light available for photosynthesis in submerged aquatic plants is a function of the water quality, as light is absorbed and scattered by water and suspended particulate matter. Phytoplankton impose a negative feedback on their own productivity, since the accumulation of cells absorbs and blocks more sunlight. The supply rate of nutrients also determines the rate of primary production. Phytoplankton absorb nutrients at a rate that asymptotically approaches a maximum as the nutrient concentration in the water increases (Valiela, 1991).

PRIMARY CONSUMERS: THE CRAYFISH

Crayfish are omnivorous and eat both living and dead organisms (Hobbs, 1989; McClain et al., 1998). As the macrofaunal organism in our system, the crayfish's health was the most visible indicator of the health of the entire physical mesocosm. Certain water quality parameters influence the health and growth of the crayfish. These include temperature, dissolved oxygen, calcium ions, pH, and ammonia concentration.

Temperature

The optimum water temperature for pond–raised crayfish ranges from 22°C to 27°C. This range optimizes the molting process and metabolic rates, and affects oxygen production from photosynthesis of aquatic plants (Huner and Lindqvist, 1995). Additionally, oxygen solubility varies greatly with temperature (Snoeyink and Jenkins, 1980). To simplify the modeling process, a constant temperature of 22°C ±2°C was maintained throughout the study by housing the crayfish mesocosms in a room that does not experience major temperature fluctuations.

Dissolved Oxygen (DO)

For an optimal molting period of the crayfish, the DO should remain above 2.0 mg L^{-1} (Nyström, 2002). When the dissolved oxygen levels fall below 5.0 mg L^{-1}, aquatic life is considered under stress (Huner and Lindqvist, 1995). In the physical mesocosm, the dissolved oxygen concentrations ranged from 4 to 8 mg L^{-1}, with occasional drops to the 2 mg L^{-1} range. No mortalities occurred due to the very low DO levels. However, the crayfish responded to low DO levels by moving to the water's surface.

Calcium Ions

Calcium ion concentration in the tissues of the crayfish influences length, body weight, and physiological robustness. The calcium ion concentration was monitored as the alkalinity and needed to be at least 20 mg L^{-1} (as calcium carbonate) (Adegboye, 1981). In the physical, self–sustaining mesocosm, the alkalinities remained above 55 mg L^{-1}.

These values were maintained by the addition of crushed coral to the gravel.

pH

Typically, aquatic life functions best in a pH of 6 to 9 (Wheaton, 1977). The buffering capacity of the water in the physical mesocosm was due, primarily, to the salts of weak acids, although strong or weak bases may have contributed. The major portion of this capacity (measured as alkalinity) resulted from the presence of hydroxide (OH$^-$), carbonate (CO$_3^{2-}$), and bicarbonate (HCO$_3^-$), listed here in order of their association with high pH values (Sawyer et al., 1994). In the physical mesocosm, the pH typically ranged from 6.5 to 7.5. The virtual mesocosm considered both the pH and the buffering capacity of the system.

Ammonia

In high concentrations, ammonia can be toxic to most forms of aquatic animal life. High ammonia concentrations in water resulted from the excretion of metabolic wastes from animals (Varley and Greenaway, 1994). In the physical mesocosm, the ammonia levels varied widely, ranging from near 0 to 2.75 mg L^{-1}.

DECOMPOSERS: THE BACTERIA

Within the sealed mesocosms, plants, algae, and crayfish generated both nitrogenous (particularly ammonia) and carbonaceous waste (Brock et al., 1991). In order for a closed mesocosm to survive, the full nitrogen cycle must be established and equilibrium must be maintained between nitrification and denitrification rates and between the rates of oxygen and carbon dioxide production and consumption. Within the mesocosm, the decomposers utilized these waste products as an energy source. The bacteria responded rapidly (typically in the time frame of a few days) to excess ammonia.

Nitrifying bacteria are an integral part of the nitrogen cycle. One group of microorganisms oxidizes the ammonia to nitrite (NO$_2^-$), while another group oxidizes the nitrite to nitrate (NO$_3^-$). The former group includes *Nitrosomonas europaea*, *Nitrosomonas monocella*, *Nitrosococcus*, and *Nitrosopira*, while the latter group includes *Nitrobacter agile*, *Nitrobacter winogradsky*, and *Nitrocystis* (Koops and Moller, 1992). Using ammonium ions as electron donors and a nitrogen source and carbon dioxide as a carbon source, the nitrifiers oxidize NH$_4^+$ to NO$_2^-$ and NO$_3^-$, reducing the toxicity of the nitrogen compound buildup in the aquatic systems (Holdich and Lowery, 1988). Denitrifiers, such as *Alcaligenes*, *Achromobacter*, *Micrococcus*, and *Pseudomonas*, reduce nitrate to gaseous N$_2$O, NO and N$_2$ (Grunditz, 1999).

Heterotrophic bacteria, decomposers present on the bottom substrate in aquatic systems, consume organic waste material excreted by the crayfish and produce carbon dioxide and water. Organic material serves as an electron donor and carbon source during heterotrophic respiration. Heterotrophs also obtain nitrogen from NH$_4^+$ to perform this metabolic process and transform the carbon found in particulate waste from the crayfish into a form (carbon dioxide) used by plants for photosynthesis (Metcalf and Eddy, 1979).

Several types of microorganisms were included in the virtual mesocosm, including both aerobes and anaerobes. Respiration of aerobic bacteria required the presence of

oxygen to serve as an electron acceptor and, consequently, was a source of oxygen depletion. The aerobic bacteria that were simulated included nitrifiers (autotrophs) and heterotrophs. Denitrifying bacteria were the only anaerobic microorganisms included in the virtual mesocosm. The overall cell composition in the model was approximated as $C_5H_7O_2N$ (Grady et al., 1999).

MODEL DEVELOPMENT

THE MODEL

The virtual mesocosm was modeled using a series of coupled first–order differential equations. These equations were implemented and solved using the Stella graphical systems modeling package. Stella models utilized user–defined *stocks* (state variables), which are acted upon by input and output flows. The rates of flows are modified by *converters*, which are defined by the flow rate coefficients, information flows from the state–variables, governing equations, etc. (Hannon and Ruth, 1997). The state variables selected for the Stella model mesocosm were anacharis biomass, alfalfa biomass, crayfish biomass, water, oxygen, nitrogen, carbon dioxide, organic carbon, carbonate, bicarbonate, total ammonia, total nitrite, and total nitrate. To enhance the overview of the model and to ease troubleshooting, cohesive model components were combined into *sectors*. Thus, for example, the equations describing the feeding and growth rates of the crayfish were grouped together in a single sector.

GENERAL ASSUMPTIONS

Whether in nature or enclosed in a small tank, ecosystems are extremely complex systems of individuals or populations interacting through the transfer of matter and energy and through positive and negative feedbacks loops. The following simplifying assumptions were made to aid the development of the Stella model:
- Water level in the tank, once defined, remained constant.
- Light levels remained constant and were not limiting to the system.
- The temperature of the mesocosm remained constant at 22°C.
- The release of ammonia to the air was negligible.
- The air pressure was one standard atmosphere.
- The crayfish consumed food at a constant rate per unit crayfish biomass as long as food was available. The crayfish did not eat each other unless the supply of plant biomass was depleted.
- The crayfish grew logistically to a maximum size.
- The gravel substrate was uniformly covered by bacterial biofilm. Thus, the total bacterial biomass in the system was constant.
- Anacharis and alfalfa have a biomass composition similar to that of algae. Thus, the independent growth of algae did not significantly affect the simulation.

STATE EQUATIONS

Following the assumptions listed above, the virtual mesocosm was programmed into Stella. The differential equation describing each state variable was programmed independently. These state variables were linked by the various flows specified by the ecological relationships. The magnitude of these flows was specified using the equations below and information flowing from the various state variables. The overall model structure is shown in figure 1. The individual state equations and calculations are discussed below.

THE CRAYFISH

The crayfish were implemented as a group of sectors. The following sectors were set up: crayfish oxygen consumption, feeding and growth rates, carbon dioxide and ammonia production, and carbonaceous waste production. The state variable describing the mass of the crayfish was used to specify the converters describing the growth rate, food, and oxygen consumption.

Oxygen Consumption

According to Armitage and Wall (1982), crayfish oxygen consumption is directly affected by temperature. As temperature increases, metabolic oxygen consumption increases. For a crayfish that is starved, the consumption rate of oxygen decreases. Additionally, oxygen solubility varies greatly with temperature, affecting the proportioning between the aqueous and gaseous phases. For 10 g of crayfish at 22°C, the oxygen consumption was described as:

$$125 \times 10^{-6} \, [\text{L/h}] \cdot 24 \, [\text{h/day}] \cdot 0.001 \, [\text{m}^3/\text{L}] \cdot$$
$$1.2929 \times 10^3 \, [\text{g/m}^3] = 0.038787 \, [\text{g O}_2/\text{day}] \quad (1)$$

When normalized by the weight of crayfish, an oxygen consumption of 0.003879 g oxygen day^{-1} g^{-1} crayfish resulted (Armitage and Wall, 1982), which is the value used in the virtual mesocosm. By comparison, Villarreal (1990) presents a function for oxygen consumption at the same temperature that yields a normalized oxygen consumption rate of 0.00273 g oxygen day^{-1} g^{-1} crayfish.

Feeding and Growth Rates

According to Huner et al. (1975), the daily food consumption for a healthy crayfish is 3% of the crayfish's mass. In our mathematical model, the consumption rate was set to be 3.5% using data collected from the physical model. The crayfish growth rate was determined to be a constant rate of 0.031 g day^{-1}. The use of an average rate of weight gain was an approximation, since the rate of weight gain was nonlinear. A significant change in weight occurred immediately following a molt. Slower rates of change occurred between molts. However, since our system contained multiple crayfish, the total crayfish biomass increased at a more linear rate. A loss of crayfish biomass was assumed to occur through death by cannibalism. Cannibalism was assumed to only occur when the total plant biomass dropped to zero.

Carbon Dioxide and Ammonia Production

The production of carbon dioxide was calculated using the general formula for respiration (Novotny and Olem, 1994):

$$C_{106}H_{180}O_{45}N_{16}P + 53(1/4)H_2O \rightarrow$$
$$47(1/8)CO_2 + 58(7/8)CH_4 + 16NH_3 + H_3PO_4 \quad (2)$$
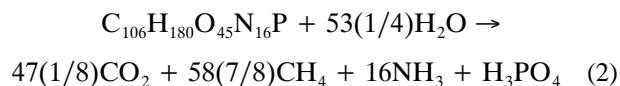
The ammonia production was calculated using a waste production model for fish (Jorgensen, 1983):

$$NH_3 \, [\text{g}] = 1.8 \cdot \text{oxygen consumed} \, [\text{g}] \quad (3)$$

Carbonaceous Waste Production

A carbon mass balance was created to estimate the organic waste produced by a crayfish:

$$C_{in} - C_{out\ respiration} - C_{growth} = C_{waste} \qquad (4)$$

Using the food consumption required by a healthy crayfish and an average molecular composition of plant biomass ($C_{106}H_{180}O_{45}N_{16}P$), crayfish carbon intake was calculated to be:

$$C_{in} = 0.035 \cdot (\text{crayfish [g]}) \cdot$$

$$(1272\ [\text{g carbon}] / 2443\ [\text{g plants}]) \qquad (5)$$

The percentage of carbon in a crayfish body was assumed to be 5.25% of wet weight (Musgrove and Geddes, 1995) and the growth rate was 0.031 day^{-1}. Using the generalized respiration equation (eq. 2), the following equation was solved:

$$C_{out\ respiration} = C_{released\ as\ CO2} + C_{released\ as\ CH4} \qquad (6)$$

ANACHARIS

In the simulation, anacharis biomass was tracked as a state variable, with an inflow of growth and an outflow of consumption by crayfish. It was assumed that the chemical makeup of the anacharis biomass followed the molar ratios of 106: 46: 16 for carbon, oxygen, and nitrogen, as it does in phytoplankton (Day et al., 1989; Redfield et al., 1963). These ratios were used to calculate the molar uptake of these constituents from the water as the anacharis grew.

Anacharis Growth

The growth of the anacharis was modeled as a first–order growth expression by calculating a total relative growth rate (RGR), which related the rate of new biomass production per unit of standing biomass according to the following equation (Thornley, 1976):

$$dW/dt = RGR \cdot W \qquad (7)$$

where
dW/dt = total growth rate [g day^{-1}]
W = dry weight of plant biomass [g]
RGR = total relative growth rate [day^{-1}].

The total relative growth rate was modeled as the product of two rates: the RGR as a function of the ammonia concentration, and the RGR as a function of the carbon dioxide concentration.

The relative growth rate as a function of the ammonia concentration was modeled according to the logistic relationship (Thornley, 1976):

$$RGR_{NH_4} = RGR_{max} \left[1 - \left(\frac{RGR_0}{RGR_{max}} \right)^{(1-N/\Gamma)} \right] \qquad (8)$$

where
RGR_{max} = maximum growth rate
RGR_0 = growth rate at zero plant tissue nitrogen
N = nitrogen content of the anacharis tissue
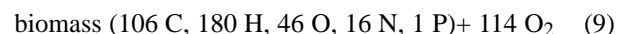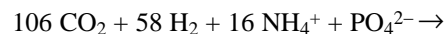Γ = nitrogen concentration producing zero growth.

This equation has been shown to fit empirical data relating the growth rate to external nitrogen content. The tissue nitrogen concentration needed to sustain the biomass but

produce zero growth has been calculated from experimental data to be 560 µmol N g^{-1} dry weight. This was used as the value for Γ in the model. The value of RGR_0, the growth rate at zero tissue nitrogen, was calculated from empirical data to be –0.1372 day^{-1}. The maximum growth rate of anacharis has been found to be 0.045 day^{-1}, as tissue nitrogen concentration was increased (Thornley, 1976). The tissue nitrogen concentration has been shown to increase nearly linearly with increasing nitrogen concentration of the surrounding water (Madsen and Baattrup–Pedersen, 1995; Madsen et al., 1998). The anacharis tissue nitrogen concentration has also been shown to increase with increasing external inorganic carbon availability. However, the increase in tissue nitrogen has been shown to be only 7% to 18% higher at 430 µm than at 17 µM nitrogen in the surrounding water. Empirical data from Madsen et al. (1998) was used to relate the tissue nitrogen concentration with the external solution nitrogen concentration. This external nitrogen was calculated in the model as the sum of the ammonia and nitrate concentrations.

The second part of the growth rate calculation involved the relationship between anacharis growth and external carbon availability. Photosynthetic rates of submerged aquatic plants have been shown to vary with external dissolved inorganic carbon concentrations. The rate of photosynthesis has been shown to increase proportionally with the inorganic carbon concentration, but leveled off once sufficiently high concentrations were reached (Madsen and Sand–Jensen, 1991). While submerged macrophytes have been shown to utilize both carbon dioxide and bicarbonate as their source of inorganic carbon, it has also been shown that macrophytes exhibit a greater affinity for CO_2 than for HCO_3^- (Allen and Spence, 1981). Therefore, the dependence of growth rate on carbon availability was modeled using a Michaelis–Menten formulation relating the concentration of carbon dioxide with a K_m of 0.30 mol m^{-3} (Allen and Spence, 1981; Madsen and Sand–Jensen, 1991). The formulation in the model assumed that all of the carbon for the growth of the plant was taken from the available carbon dioxide. These levels were multiplied by the growth rate calculated for the nitrogen limitation to give the total growth rate of the anacharis day^{-1}.

Photosynthesis and Respiration

Photosynthesis and respiration by the anacharis were modeled according to the general equation for net productivity (Redfield et al., 1963):

$$106\ CO_2 + 58\ H_2 + 16\ NH_4^+ + PO_4^{2-} \rightarrow$$

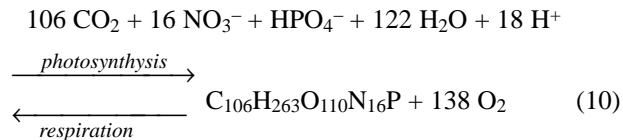$$\text{biomass (106 C, 180 H, 46 O, 16 N, 1 P)} + 114\ O_2 \qquad (9)$$

This equation was used to calculate the net consumption of carbon dioxide and ammonia, and the net production of oxygen as the anacharis grew. These were programmed into the model as stoichiometric ratios that contributed to the state variables, tracking the carbon dioxide, ammonia, and oxygen as appropriate.

ALFALFA

To help maintain air quality and to provide additional food supply for the crayfish, alfalfa (*Medicago sativa*) was maintained in the tank. The mass of the alfalfa was tracked as a state variable. Though consumption of the calcium–containing alfalfa might promote crayfish growth, the major

effect of introducing alfalfa to the closed self–sustaining mesocosms was its simultaneous adjustment of the total oxygen and carbon dioxide in the crayfish biosphere due to photosynthesis and respiration.

To simplify the complex chemical reactions, the relationship among the mass of alfalfa and the mass of oxygen released to the environment and carbon dioxide consumed by the respiration process was described by the equation (Stumm and Morgan, 1996):

$$106\ CO_2 + 16\ NO_3^- + HPO_4^- + 122\ H_2O + 18\ H^+$$

$$\xrightarrow[respiration]{photosynthesis} C_{106}H_{263}O_{110}N_{16}P + 138\ O_2 \qquad (10)$$

The initial amount of alfalfa, in grams, was user specified. The average growth rate of alfalfa was calculated as 0.01253 g day^{-1} plant^{-1} (Teutsch et al., 2000). The produced oxygen and consumed carbon dioxide amounts were modeled from this rate. The consumption of alfalfa by the crayfish was included in the alfalfa model as well. The ratio of alfalfa to anacharis eaten by crayfish per day was user specified. These changes in the mass of alfalfa affected the production of oxygen and the consumption of carbon dioxide. The changes, in turn, altered the total oxygen and carbon dioxide in the air and resulted in changes to the associated sectors.

BACTERIA

Multiple sectors were used to model bacterial activity in the tanks. The total amounts of ammonia, nitrite, nitrate, and organic carbon were tracked as state variables. Inflows to the state variables included nitrogenous waste produced by the crayfish and nitrification products of that waste (nitrite and nitrate). Bacterial activity (e.g., ammonia transformation) and plant uptake subtracted from the state variables and were represented as outflows.

Preliminary Calculations

Using empirical data available from five physical crayfish mesocosms, calculations were performed to estimate the representative bacterial biomass and volume. A tubing fitting was placed in a control tank to provide an appropriate surface for bacterial growth. After a thick layer of biofilm accumulated, the tube was removed from the tank and cleaned with ultrasound. The mass and volume of the tube were recorded before and after cleaning. The density of the biofilm growing in these mesocosms was 0.34 g cm^{-3}.

Biofilm on the gravel in the control tank was monitored daily for 15 days. Gravel was removed from the control tank and its mass was recorded. The mass of the biofilm found on the gravel was obtained by cleaning the gravel with ultrasound and recording the reduction in mass. The mass of biofilm remained nearly constant over time. The average amount of biofilm was 0.027 g biofilm g^{-1} gravel. Assuming the gravel was uniformly covered with biofilm, the total weight of the biofilm on the gravel was 392.4 g. The volume of biofilm was 1154 cm^3.

Nitrification

Experimental measurements of nitrite yielded the total nitrite concentration, which was an intermediate step in nitrification. Having no means to distinguish between these two concentrations, only the initial and end products of the total nitrification were considered, i.e., ammonia and nitrate. The total equation for the nitrification can be expressed as follows (Grunditz, 1999):

$$NH_4^+ + 2O_2 \rightarrow NO_3^- + 2H^+ + H_2O \qquad (11)$$
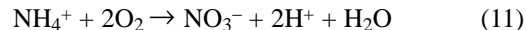
The nitrification rate in the model was described using Monod kinetics. A double substrate limiting equation was used to account for any constraints that may arise due to the microorganism's growth substrate availability as well as competition for oxygen among all of the aerobic bacteria and crayfish. The substrate utilization rate can be described (Jorgensen and Gromiec, 1989) using:

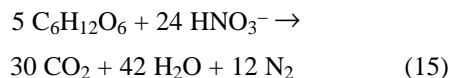$$dS_n/dt = \mu_n \cdot X_n/Y_n \qquad (12)$$

and

$$\mu_n = \mu\max_n \cdot \left[\frac{S_n}{Ks_n + S_n}\right] \cdot \left[\frac{DO}{Kso_n + DO}\right] - Kd_n \qquad (13)$$

where

μ_n = specific growth rate of nitrifying bacteria [day^{-1}]

$\mu\max_n$ = maximum specific growth rate of nitrifying bacteria, 0.001 [day^{-1}] (Wynn and Liehr, 2001)

S_n = concentration of ammonia–N in the system [mg L^{-1}]

DO = dissolved oxygen concentration in the system [mg L^{-1}]

Ks_n = half saturation constant for ammonia–N, 1.2 [mg L^{-1}] (Jorgensen and Gromiec, 1989)

Kso_n = half saturation constant for dissolved oxygen, 1.0 [mg L^{-1}] (Wynn and Liehr, 2001)

Kd_n = endogenous decay coefficient for nitrifying bacteria, 0.002 [day^{-1}] (Wynn and Liehr, 2001)

Y_n = cell yield of nitrifying bacteria, 0.06 [mg bacterial cells produced per mg ammonia–N oxidized] (Jorgensen and Gromiec, 1989)

X_n = concentration of ammonia oxidizing bacteria in the system [mg L^{-1}].

Denitrification

Denitrification is the reduction of nitrate to gaseous nitrogen compounds by facultative anaerobic bacteria (Focht and Verstraete, 1977) and followed the general chemical equations (Day et al., 1989):

$$C_6H_{12}O_6 + 6\ HNO_3^- \rightarrow 6\ CO_2 + 9\ H_2O + 3\ N_2O \qquad (14)$$

$$5\ C_6H_{12}O_6 + 24\ HNO_3^- \rightarrow$$
$$30\ CO_2 + 42\ H_2O + 12\ N_2 \qquad (15)$$

For simplification of the model development, it was assumed that all denitrification followed the second pathway outlined in equation 15, resulting in an accumulation of nitrogen gas. In addition, denitrification was assumed to take place at the same rate on each piece of gravel in the aquarium. As a working value, we used a denitrification rate of 22.7 mg N m^{-2} day^{-1} (Jannasch and Williams, 1985). This value was estimated using data from several locations in the U.S. and Europe. The denitrification rate was expressed as a Michaelis–Menten relationship related to the nitrate and reductant concentrations (Focht and Verstraete, 1977):

$$-\frac{dN}{dt} = \frac{V_{max} \cdot (NO_3^- - N) \cdot (\text{reductant})}{K_n + (NO_3^- - N) \cdot (\text{reductant}) + K_c} \quad (16)$$

An average value of V_{max} was found to be 1.02×10^{-5} mol NO_3^-–N mL^{-1}. Further, Focht and Verstraete (1977) used a reductant: NO_2^-–N ratio of 2 to 3. An average of 2.5 was therefore used in this model. Thus, the concentration of reductant was 2.45×10^{-5} mol cm^{-3} day^{-1}. The molarities for K_n and K_c were found to be 1.21×10^{-5} mol NO_3^-–N cm^{-3} and 3.57×10^{-5} mol NO_3^-–N cm^{-3}, respectively. Denitrification and nitrification were assumed to take place close to or on the biofilm; therefore, concentrations were converted to moles with respect to the volume of biofilm.

Heterotrophs

Heterotrophic bacteria were modeled according to the following general equation (Metcalf and Eddy, 1979):

$$C_6H_{12}O_6 + 6\,O_2 \rightarrow 6\,CO_2 + 6\,H_2O \quad (17)$$

A carbon mass balance was performed on the crayfish to obtain an approximation of the mass of organic material excreted into the system. An estimate of the total amount of heterotrophic bacteria present was obtained using a typical ratio of autotrophic to heterotrophic bacteria found in a freshwater stream (Lozano, 1999). Using Monod kinetics, the substrate utilization rate was calculated using:

$$dS_h/dt = \mu_h \cdot X_h/Y_h \quad (18)$$

and

$$\mu_h = \mu\,max_h \cdot \left[\frac{S_h}{K_{s,c} + S_h}\right] \cdot \left[\frac{DO}{K_{s,oh} + DO}\right] - K_{dh} \quad (19)$$

where

μ_h = specific growth rate of heterotrophic bacteria [day^{-1}]

μmax_h = maximum specific growth rate of heterotrophic bacteria, 9 [day^{-1}] (Rittmann, 1987)

S_h = concentration of total organic carbon in the system [mg L^{-1}]

DO   = dissolved oxygen concentration in the system [mg L^{-1}]

$K_{s,c}$ = half saturation constant for organic carbon, 50 [mg L^{-1}] (Wynn and Liehr, 2001)

$K_{s,oh}$ = half saturation constant for dissolved oxygen, 1.0 [mg L^{-1}] (Wynn and Liehr, 2001)

K_{dh} = endogenous decay coefficient for heterotrophic bacteria, 1.0 [day^{-1}] (Wynn and Liehr, 2001)

X_h = concentration of heterotrophic bacteria [mg L^{-1}]

Y_h = cell yield of heterotrophic bacteria, 0.6 mg bacterial cells produced per [mg organic carbon oxidized] (Metcalf and Eddy, 1979).

BICARBONATE SYSTEM

The effects of a bicarbonate buffering system on the self–sustained mesocosm were included in the model. This was considered an important goal since the pH of aquatic systems has an integral role in the behavior of abiotic components of the system. In this simulation, the buffering system was influenced solely by the production or assimilation of carbon dioxide through crayfish respiration and primary production, respectively. In the simulation, the

addition or removal of carbon dioxide directly affected the amount of total inorganic carbon (C_T) present in the system. The relative amounts of each form of inorganic carbon (H_2CO_3, HCO_3^-, and CO_2) were dependent upon the current pH of the system (Stumm and Morgan, 1996). The C_T changed over time due to both the carbon dioxide flux and the amount of carbonate (CO_3^{2-}) found in aqueous form at each pH. Since the crushed coral in the physical mesocosms was in excess, the assumption was made that the CO_3^{2-} was always present at its maximum potential. Depending on the pH of the water at any given time, the molar concentration of total carbon found in the form of CO_3^{2-} was determined by the following equation (Bialkow, 2001):

$$\log(CO_3^{2-}) = 0.0574 \cdot (pH)^2 - 1.450 \cdot pH + 4.972 \quad (20)$$

The quantities of carbonic acid (H_2CO_3) and bicarbonate (HCO_3^-) were calculated as a function of the relative percentages of the amount of inorganic carbon represented by the individual species (a function of pH) and C_T not in the form of CO_3^{2-}.

The equation for the inorganic carbon in the form of H_2CO_3 is:

$$H_2CO_3 = \left(C_T + CO_2\,flux - CO_3^{2-}\right) \cdot \left[\frac{\alpha_0}{\alpha_0 + \alpha_1 + \alpha_2}\right] \quad (21)$$

The variables α_0, α_1, and α_2 are the percentages of total inorganic carbon found in the form of H_2CO_3, HCO_3^-, and CO_3^{2-}, respectively (Stumm and Morgan, 1996). Similar equations were used to describe the partitioning of the other forms of inorganic carbon within the system. The percentage of CO_3^{2-} (α_2) was calculated as the amount of CO_3^{2-}, computed in equation 20, divided by C_T. The amounts of HCO_3^- and H_2CO_3 were calculated as C_T not in the form of CO_3^{2-}, multiplied by the total percentage of the form of interest, divided by the sum of the percentages of both forms. In addition, any changes to the quantity of CO_2 were allocated into these two compartments.

The pH was then computed using the new amounts of each individual species of inorganic carbon. As would be expected in a natural buffering system, the simulation's buffering system had a stabilizing effect on the virtual mesocosm's pH. This stabilization resulted primarily from the relationship that described the amount of CO_3^{2-} as a function of pH. As the system's pH became acidic, more CO_3^{2-} was solubilized and a greater percentage of C_T existed in the form of CO_3^{2-}. This shift caused an increase in pH. The reverse was true when the pH became basic. As the pH increased, less CO_3^{2-} existed in solution, resulting in a drop in the pH (Stumm and Morgan, 1996).

GASES IN THE MESOCOSM

The main gases in the virtual mesocosm included carbon dioxide, nitrogen, and oxygen. These three gasses were handled using a similar approach and set of equations. Initial conditions for each of the gases were calculated based on their physical chemistry. The partitioning of the gases between the aquatic and atmospheric portions of the closed mesocosm determined the initial conditions and the changes in these conditions over time.
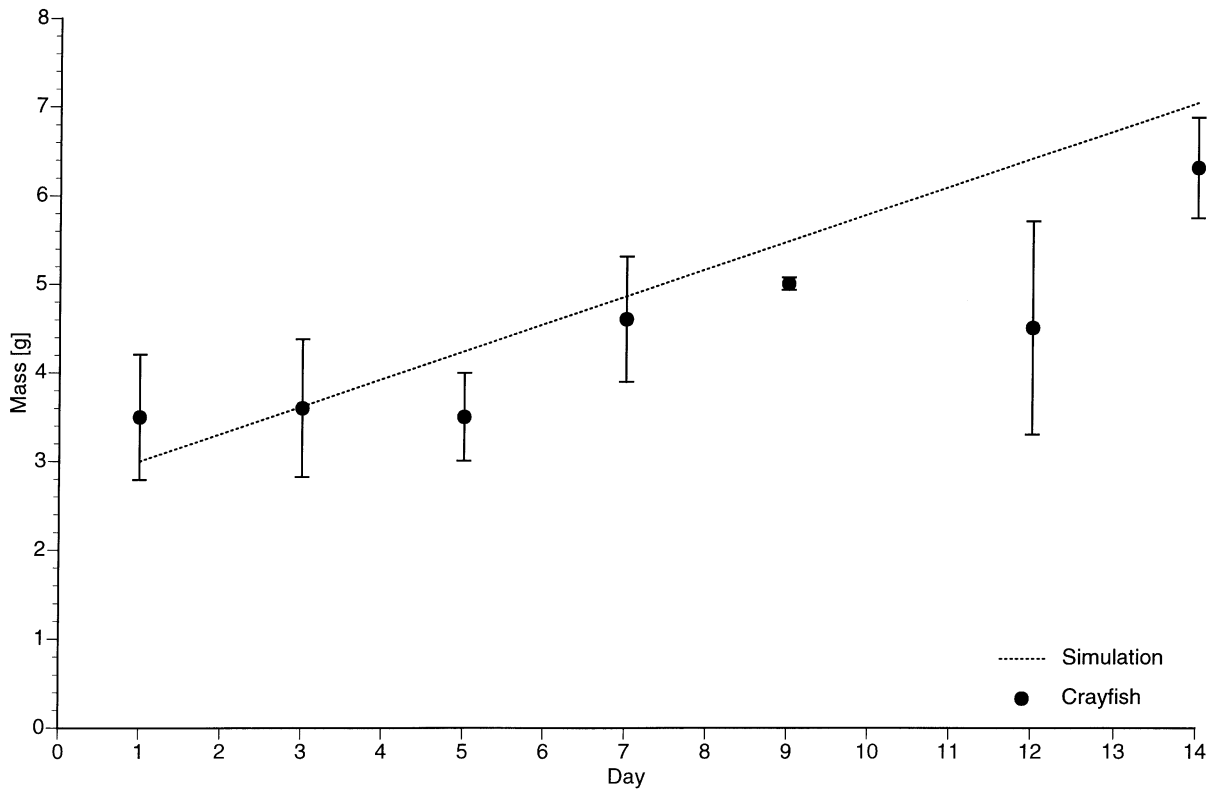
Figure 2. Crayfish mass as a function of time during optimum living conditions. Both actual and virtual data are displayed. The virtual data plotted represent a crayfish with an average starting mass (3.0 g). Error bars represent one standard deviation.

Initial Aqueous Gas Concentration

Henry's law specifies the relationship for the solubility of a gas in a liquid (McQuarrie and Rock, 1987). The partial pressure of each gas is:

$$P_{gas} = \frac{K_h \cdot n_w}{V_w \cdot P_{gas\,total}} \qquad (22)$$

where

K_h = Henry's law constant for the particular gas at a given temperature

n_w = number of moles of the gas in the water

V_w = water volume.

Because most gases obey the ideal gas law at atmospheric pressure, the pressure was purely a function of gas moles, volume, and temperature. Holding temperature constant, the following relationship was derived:

$$\frac{n_{air}}{n_w} = \frac{K_h \cdot V_A}{R \cdot T \cdot V_W} \qquad (23)$$

where

n_{air} = number of moles of gas in the air

V_a = volume of the air space

R = gas constant

T = absolute temperature.

Because the total moles of gas equaled the sum of the moles of gas in the water and the air:

$$\frac{n_{total} - n_w}{n_w} = \frac{K_h \cdot V_a}{R \cdot T \cdot V_w} \qquad (24)$$

therefore:

$$n_w = \frac{n_{total}}{\left(\dfrac{K_h \cdot V_a}{R \cdot T \cdot V_w} \right) + 1} \qquad (25)$$

Given the total number of moles of a gas in a closed mesocosm and the relative volumes of the air and water partitions, the total number of moles of gas that remained dissolved in the water was calculated using equation 25. The number of moles in the air was the total moles of the gas minus the moles that remained in the water.

For example, the initial number of moles of gaseous nitrogen was calculated using the air space volume and the ideal gas law. The initial concentration of nitrogen in the aqueous phase (moles cm^{-3}) was computed from the concentration of nitrogen in the gaseous phase using Henry's law and a Henry's law constant of 1.6×10^6 atm mol^{-1} cm^{-3}. All changes in the nitrogen were calculated as deviations from the initial conditions, with the distribution between the aqueous and the vapor phases computed using Henry's law.

The final product of the denitrification was assumed to be nitrogen (N_2) and accumulated in the state variable for nitrogen. Using Henry's law, the nitrogen was partitioned into nitrogen in the air and water phase. The number of moles of gas was calculated noting that (at standard temperature and pressure) one mole of molecular gas will occupy 22,400 cm^3. Correcting for the 22°C mesocosm temperature yielded the number of moles of nitrogen in the air.
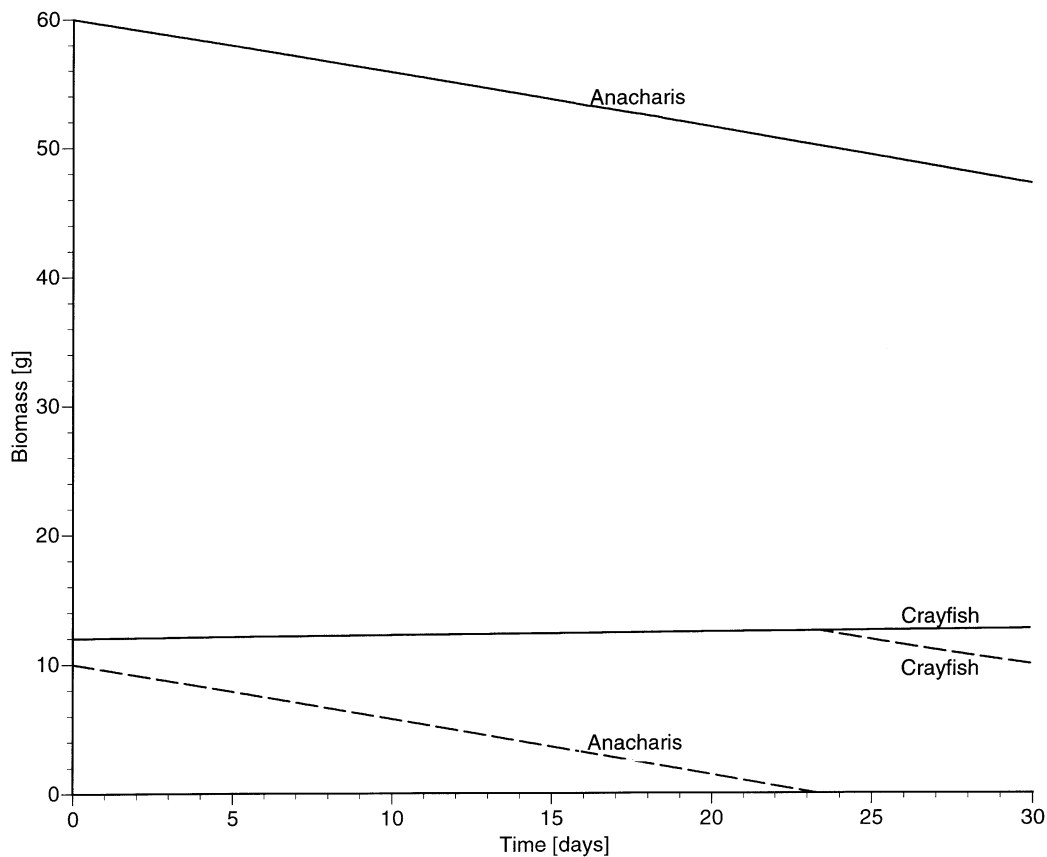
Figure 3. Crayfish mass as a function of time. The upper curve (solid line) shows crayfish growth (g) when starting with adequate anacharis (60 g), 1 alfalfa plant cm^{-2}, and no alfalfa consumption. Under these initial conditions, the crayfish biomass continuously increases. The lower curve (dashed line) shows crayfish growth (g) when starting with insufficient anacharis to last for a month (10 g) and no alfalfa consumption. Under these conditions, the crayfish biomass decreases linearly, due to cannibalism, once the anacharis is completely consumed.

RESULTS AND DISCUSSION

To evaluate simulation performance, the virtual mesocosm's output was compared to trends found in the physical mesocosm (Schreuders et al., 2002). Where test results from the physical mesocosm were not applicable or not available, published values found in the literature were used. Many parameters contributed to the balancing act of the ecosystem. A number of sensitivity analyses were generated emphasizing different parts of the system. Overall, the virtual mesocosm behaved correctly where expected, with trend rates of the various accumulators following expected results.

CRAYFISH

Typical crayfish growth, under non–stressed conditions, is shown in figure 2. Data collected from the actual mesocosms is plotted with results obtained from the virtual model, which was run using an initial crayfish mass of 3.0 g (average for a crayfish used in this study). The model adequately predicts actual crayfish growth under favorable conditions. It should be noted that the growth rate of an individual crayfish is nonlinear, with larger weight increases occurring during molting. However, when the aggregate growth rate of several crayfish is considered, the molts occur asynchronously, resulting in more linear rate of weight increase. Under stressed water quality conditions, due to low food supply, the model predicts a linear decrease in crayfish mass, as depicted in figure 3. Actual mesocosm data for this scenario was

unavailable for comparison with the virtual data. A circumstance that the model does not accurately predict is the event of crayfish molting. Actual data collected from the mesocosms indicate crayfish growth deviates from linearity, which has not been worked into the model.

PLANTS

The initial mass of anacharis affected certain water quality parameters. For example, at low initial anacharis biomass, the model showed ammonia concentrations reaching dangerously high levels. Crayfish consumption rate was greater than the growth rate of anacharis, which greatly decreased the amount of ammonia absorbed by plants. In addition, low plant mass caused a low dissolved oxygen concentration in the virtual mesocosm, which slowed or stopped nitrification and allowed for ammonia accumulation in the system. As shown in figure 4, the initial mass of anacharis in the enclosed ecosystem also determined whether a healthy dissolved oxygen level was achieved. The model was run assuming three average crayfish were placed in the mesocosm (total mass 9.0 g). Sealing the mesocosm with only 10 g of anacharis caused the oxygen level to rapidly drop, and the system crashed. According to the virtual model, 60 g of anacharis is the absolute minimum amount of anacharis with which one could start a sealed mesocosm and expect an acceptable dissolved oxygen concentration. The students building the actual mesocosms used this information when planning their mesocosm design and all started with an
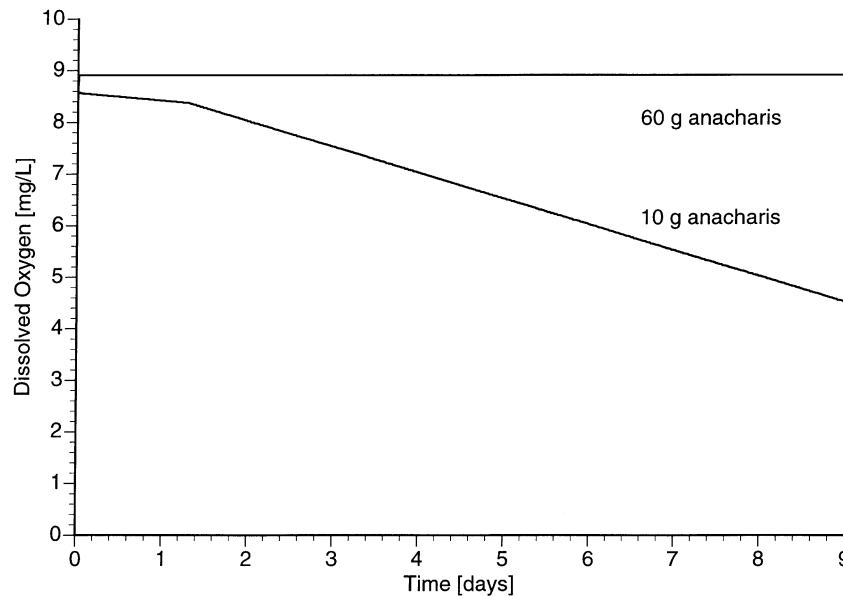
Figure 4. Dissolved oxygen concentration in the aqueous phase of the virtual mesocosm under two different initial conditions for the plants. In the upper curve, sufficient anacharis is present that the dissolved oxygen concentration remains near saturation. In the lower curve, the anacharis is consumed by the crayfish at a rate faster than it grows, and the oxygen steadily decreases.

anacharis mass in excess of 100 g. Alfalfa also affected water quality parameters but had less of an effect on the whole system than anacharis. When the rate of consumption of alfalfa by the crayfish was zero, the alfalfa grew in a linear fashion. The consumption of carbon dioxide and production of oxygen by the alfalfa likewise increased linearly. The carbon dioxide consumed was subtracted from the total carbon dioxide in the system, and the oxygen produced was added to the total systemic oxygen. When the crayfish consumption rate of the alfalfa exceeded its growth rate, the total levels of alfalfa, carbon dioxide consumption by alfalfa, and oxygen production by the alfalfa decreased linearly.

Certain aspects of alfalfa consumption were not addressed in this simulation. For example, the crayfish growth rate would be expected to increase due to the consumption of alfalfa. Due to the high calcium consumption of crayfish, the calcium carbonate solubility potentially would be influenced and the water quality of the system would be further affected. However, this would be the case only if $CaCO_3$ was not present in excess. Since oxygen produced during photosynthesis was used by the oxygenase activity, glycolate oxidase, respiration, and other processes, only the remainder of the oxygen was released to the environment.

BACTERIA

Calibration was an important step in creating the bacterial portion of the virtual mesocosm. Any constants required in the Monod model were first taken from values typically used in modeling aerobic biological treatment (Rittmann, 1987). In an attempt to create a virtual mesocosm more consistent with the physical mesocosm rather than wastewater treatment, values used to model wetlands were also considered (Wynn and Liehr, 2001).

The simulation satisfactorily predicted the ammonia concentration inside the mesocosms for most iterations of the physical mesocosm. In figure 5, actual mesocosm data is plotted with the model output showing ammonia concentration over time. The initial ammonia concentration used to run the simulation was taken from the physical mesocosm. Ammonia levels in the simulation quickly dropped as nitrification took place. The steady–state ammonia level established at about 0.2 mg L^{-1}, a relatively safe level for aquatic life. Nitrifying bacteria may have appeared too efficient in the simulation due to overestimation of the initial amount of nitrifying bacteria present in the system or failure to account for stresses outside ammonia and oxygen availability (e.g., pH fluctuations).

The virtual mesocosm successfully estimated the organic carbon concentration (fig. 5). Initial organic carbon present was set at zero, since the containment tanks of the physical mesocosms were cleaned prior to each experiment. Crayfish activity started immediately, and carbonaceous waste was produced. As a result, the heterotrophic bacteria started to regulate the organic carbon present in the tanks after approximately 1 day of simulation. The total organic carbon concentration approached steady–state, producing an average value between 6 and 7 mg L^{-1}. Model output was evaluated by comparing it with data available for a freshwater lake ecosystem, as actual mesocosm data was not available for this parameter. The values generated by the simulation remained between 1 and 10 mg L^{-1}, a typical range for a freshwater lake (Rittmann and McCarty, 1980).

The heterotrophic and autotrophic aerobic bacteria modeled in the current version of the crayfish virtual mesocosm appeared to yield realistic results. Anaerobic denitrifying bacteria were not altered during this iteration. A more complete model would use the same kinetic equations to describe all bacterial growth, aerobic and anaerobic, present in the enclosed mesocosm. Similarly, the general stoichiometric relationships resulting from bacterial growth and chemical transformation could be replaced with versions that are specific to the species found in the physical mesocosm. The assumption that all anacharis leaf litter was eaten by the crayfish was also a simplification. This waste accumulated in relatively large quantities on the bottom of the physical mesocosms. Unattached, dead leaves could be added to the
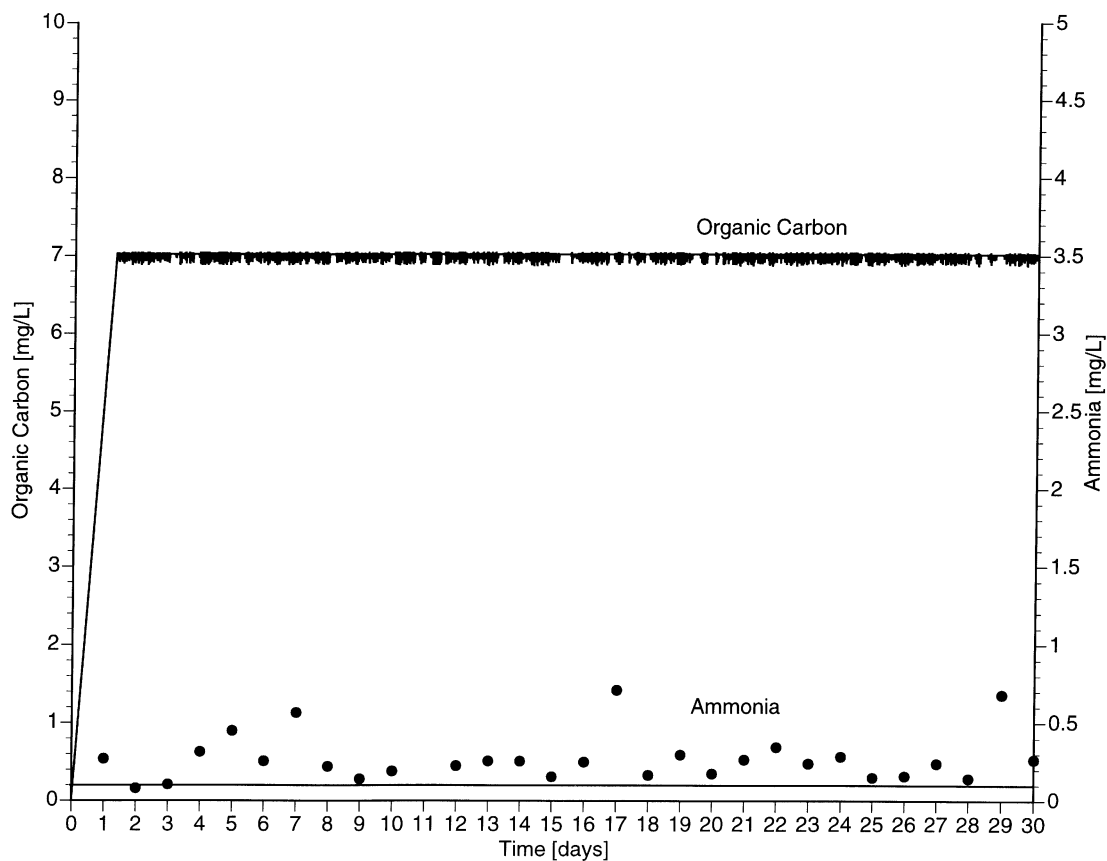
Figure 5. Concentrations of ammonia and total organic carbon in the virtual mesocosm. An initial ammonia concentration was taken from actual mesocosms and used for the virtual model. The model predicted a dramatic drop in ammonia concentration before reaching a steady–state value. Actual mesocosm ammonia concentrations are also plotted. Model predictions for total organic carbon in the system show a continual increase before reaching its steady–state value.

other carbonaceous waste, which had the potential to be degraded by heterotrophic bacteria.

WATER QUALITY

The buffering capacity module was examined in a number of different ways. Running the simulation with either an abnormally acidic or basic pH proved to be the most useful for validating the virtual mesocosm. In order to investigate how the simulation would respond to a low pH, the initial amount of H_2CO_3 was set high in comparison to the other forms of inorganic carbon, yielding a starting pH of 4.

The mathematical model of the buffering system was successful. The system responded by allowing more CO_3^{2-} to go into solution than was initially present. This rapid increase in CO_3^{2-} led to a concurrent increase in the pH. In fact, the increase was so dramatic that the system overshot equilibrium. Stabilization occurred once equilibrium was reached between the CO_3^{2-} in solution (a function of pH) and the percent of total inorganic carbon that was represented (which determines pH).

In subsequent iterations of the virtual mesocosm, the buffering module and pH can be more fully integrated with other components of the simulation. For example, in a simulation that takes into consideration the toxicity of ammonia to the crayfish, it would be important to incorporate the pH to determine what percentage of the ammonia was un–ionized and therefore bioavailable to the crayfish. The pH also has varying effects on bacterial growth, reproduction,

and degradation ability, which could potentially be incorporated into the virtual mesocosm.

There are several ways that the treatment of a buffering system could be handled within Stella. One of the simplest approaches was chosen in order to get an idea of how the different forms of inorganic carbon would be partitioned out, given certain starting parameters. While the chosen method worked well, there are different approaches that would allow a user to investigate additional aspects of the system. However, for the intended purpose of developing a self–sustaining mesocosm over the period of a month, the bicarbonate system was not the most critical aspect of the system. This statement is based on both empirical data collected from physical mesocosms, as well as the knowledge that calcium carbonate was in excess in the mesocosms.

CONCLUSIONS

Currently, the virtual mesocosm assumes absolute values for reaction coefficients, uptake rates, stoichiometric ratios in biomass, etc. Assumption of absolute values deviates from reality because, as in the integration of a number of complex biological systems, the physical mesocosms were prey to considerable random variation. In future development, many of the biological reaction coefficients currently defined as constants might instead be described by a mean value and a standard deviation, thus implementing a random component into the model.

While the mesocosm was, by definition, incompletely simulated, a number of important aspects of a natural ecosystem were integrated. A useful simulation is one that represents the most important aspects of a system, yet maintains a level of simplicity that allows the user to gain insight into the underlying mechanics of the system. Thus, this simulation can be used to enhance the understanding of the processes that take place in a sealed mesocosm. With proper calibration, the virtual mesocosm can be used as a valuable learning tool to introduce concepts of ecological interactions and to explore the sensitivity of aquatic meso-cosms to variations in parameters. Using Stella as a simulation tool provided an easy way to look into the variables that contribute to water quality, and how the entire mesocosm was balanced.

REFERENCES

Adegboye, D. 1981. Table size and physiological condition of the crayfish in relation to calcium ion accumulation. In *Proc. 5th International Symposium on Freshwater Crayfish*, 115–125. Auburn, Ala.: International Association of Astacology.

Adey, W. H., and K. Loveland. 1998. *Dynamic Aquaria: Building Living Ecosystems.* 2nd ed. San Diego, Cal.: Academic Press.

Allen, E. D., and D. H. N. Spence. 1981. The differential ability of aquatic plants to utilize the inorganic carbon supply in fresh waters. *New Phytologist* 87(2): 269–283.

Armitage, K. B., and T. J. Wall. 1982. The effects of body size, starvation, and temperature acclimation on oxygen consumption of the crayfish *Orconectes nais*. *Comp. Biochem. Physiol.* 73A(1): 63–68.

Beyers, R. J., and H. T. Odum. 1993. *Ecological Microcosms.* New York, N.Y.: Springer–Verlag.

Bialkow, S. 2001. Overheads on carbonate. Available at: www.chem.usu.edu/faculty/SBialkow/Classes/3600/Overheads/Carbonate/CO2.html.

Brock, T. D., M. T. Madigan, and J. M. Martinko. 1991. *General Microbiology.* 6th ed. Englewood Cliffs, N.J.: Prentice Hall.

Day, J. W., C. A. S. Hall, K. W. M., and A. Yanez–Arancibia. 1989. *Estuarine Ecology.* New York, N.Y.: John Wiley and Sons.

Focht, D. D., and W. Verstraete. 1977. Biochemical ecology of nitrification and denitrification. *Adv. Microbiol. Ecol.* 1: 135–214.

Grady, C. P. L., G. T. Daigger, and H. C. Lim. 1999. *Biological Wastewater Treatment.* 2nd ed. New York, N.Y.: Marcel Dekker.

Grunditz, C. 1999. Bioassays for the determination of nitrification. Dr. Tchn diss. Stockholm, Sweden: Royal Institute of Technology.

Hannon, B. M., and M. Ruth. 1997. *Modeling Dynamic Biological Systems.* New York, N.Y.: Springer–Verlag.

Hobbs, H. H. J. 1989. An illustrated checklist of the American crayfishes (Decapoda: Astacidae, Cambaridae, and Parastacidae). *Smithsonian Contributions to Zoology* 480: 1–236.

Holdich, D. M., and R. S. Lowery. 1988. *Freshwater Crayfish: Biology, Management, and Exploitation.* London, U.K.: Timber Press.

Huner, J. V., and O. V. Lindqvist. 1995. Physiological adaptations of freshwater crayfishes that permit successful aquacultural enterprises. *American Zool.* 35(1): 12–19.

Huner, J. V., S. P. Meyers, and J. W. Avault. 1975. Response and growth of freshwater crawfish to an extruded, water stable diet. In *Proc. International Symposium on Freshwater Crayfish*, 149–157. Baton Rouge, La.: Louisiana State University, Continuing Education.

Jannasch, H. W., and P. S. Williams. 1985. *Advances in Aquatic Microbiology*, Vol. 3. New York, N.Y.: Academic Press.

Jorgensen, S. E. 1983. Modeling the ecological processes. In *Mathematical Modeling of Water Quality: Streams, Lakes, and Reservoirs*, 116–149. G. T. Orob, ed. New York, N.Y.: Wiley Interscience.

Jorgensen, S. E., and M. J. Gromiec. 1989. *Mathematical Submodels in Water Quality Systems: Vol. 14. Developments in Environmental Modelling.* Amsterdam, The Netherlands: Elsevier Science.

Kangas, P. 2004. *Ecological Engineering: Principles and Practice.* Boca Raton, Fla.: Lewis Publishers.

Koops, H., and U. Moller. 1992. The lithotrophic ammonia–oxidizing bacteria. In *The Prokaryotes: A Handbook on the Biology of Bacteria: Ecophysiology, Isolation, Identification, Applications*, 2625–2637. A. Balows, ed. New York, N.Y.: Springer–Verlag.

Lozano, S. Research monitoring of the Lake Michigan ecosystem. 1999. Available at: www.glerl.noaa.gov/res/Task_rpts/cmlozano13–1.html.

Madsen, T. V., and K. Sand–Jensen. 1991. Photosynthetic carbon assimilation in aquatic macrophytes. *Aquat. Bot.* 41(1–3): 5–40.

Madsen, T. V., and A. Baattrup–Pedersen. 1995. Regulation of growth and photosynthetic performance in *Elodea canadensis* in response to inorganic nitrogen. *Func. Ecol.* 9(2): 239–247.

Madsen, T. V., P. Hahn, and J. Johansen. 1998. Effects of inorganic carbon supply on the nitrogen requirement of two submerged macrophytes, *Elodea canadensis* and *Callitriche cophocarpa*. *Aquat. Bot.* 62(2): 95–106.

McClain, W. R., J. L. Avery, and R. P. Romaire. 1998. *Crawfish Production: Production Systems and Forages.* Stoneville, Miss.: Southern Regional Aquaculture Center.

McQuarrie, D. A., and P. A. Rock. 1987. *General Chemistry.* 2nd ed. New York, N.Y.: W. H. Freeman.

Metcalf and Eddy. 1979. *Wastewater Engineering: Treatment Disposal Reuse.* 2nd ed. New York, N.Y.: McGraw–Hill.

Mitsch, W. J., and J. K. Cronk. 1992. Creation and restoration of wetlands: Some design considerations for ecological engineering. In *Advances in Soil Science*, 217–259. R. Lal and B. A. Stewart, eds. New York, N.Y.: Springer–Verlag.

Mitsch, W. J., and R. F. Wilson. 1996. Improving the success of wetland creation and restoration with know–how, time, and self–design. *Ecol. Appl.* 6(1): 77–83.

Musgrove, R. J. B., and M. C. Geddes. 1995. Tissue accumulation and the moult cycle in juveniles of the Australian freshwater crayfish *Cherax destructor*. *Freshwater Biology* 34(3): 541–558.

Novotny, V., and H. Olem. 1994. *Water Quality: Prevention, Identification, and Management of Diffuse Pollution.* New York, N.Y.: Van Nostrand Reinhold.

Nyström, P. 2002. Ecology. In *Biology of Freshwater Crayfish*, 192–235. D. M. Holdich, ed. Ames, Iowa: Iowa State University Press.

Odum, H. T., and E. C. Odum. 2000. *Modeling for all Scales: An Introduction to System Simulation.* San Diego, Cal.: Academic Press.

Parrott, L., and R. Kok. 2001. A generic primary producer model for use in ecosystem simulation. *Ecol. Model.* 139(1): 75–99.

Parrott, L., and R. Kok. 2002. A generic, individual–based approach to modelling higher trophic levels in simulation of terrestrial ecosystems. *Ecol. Model.* 154(1–2): 151–178.

Redfield, A. C., B. H. Ketchum, and F. A. Richards. 1963. The influence of organisms on the composition of seawater. In *The Sea: Ideas and Observations on Progress in the Study of the Seas*, 26–77. M. N. Hill, ed. New York, N.Y.: R. E. Krieger Publishing.

Rittmann, B. E. 1987. Aerobic biological treatment. *Environ. Sci. Tech.* 21(2): 128–136.

Rittmann, B. E., and P. L. McCarty. 1980. Evaluation of steady–state–biofilm kinetics. *Biotech. Bioeng.* 22(11): 2359–2372.

Sawyer, C. N., P. L. McCarty, and G. F. Parkin. 1994. *Chemistry for Environmental Engineering.* 4th ed. New York, N.Y.: McGraw Hill.

Schreuders, P. D., D. Blersch, A. Lomander, F. Koh, P. B. Reddy, D. and Danzy. 2002. An ecological engineering project for combined undergraduate and graduate classes. *Intl. J. Eng. Ed.* 18(5): 607–615.

Snoeyink, V. L., and D. Jenkins. 1980. *Water Chemistry.* New York, N.Y.: John Wiley and Sons.

Stella. 1997. Stella 5.1 systems modeling software. Hanover, N.H.: High Performance Systems, Inc.

Stumm, W., and J. J. Morgan. 1996. *Aquatic Chemistry: Chemical Equilibria and Rates in Natural Waters.* 3rd ed. New York, N.Y.: John Wiley and Sons.

Teutsch, C. D., R. M. Sulc, and A. L. Barta. 2000. Banded phosphorus effects on alfalfa seedling growth and productivity after temporary waterlogging. *Agronomy J.* 92(1): 48–54.

Thornley, J. H. M. 1976. *Mathematical Models in Plant Physiology: A Quantitative Approach to Problems in Plant and Crop Physiology.* New York, N.Y.: Academic Press.

Valiela, I. 1991. Ecology of water columns. In *Fundamentals of Aquatic Ecology*, 29–56. R. S. K. Barnes and K. H. Mann, eds. Boston, Mass.: Blackwell Scientific.

Varley, D., and P. Greenaway. 1994. Nitrogenous excretion in the terrestrial carnivorous crab *Geograpsus grayi*: Site and mechanism of excretion. *J. Exp. Biol.* 190(1): 179–193.

Villarreal, H. 1990. Effect of temperature on oxygen consumption and heart rate of the Australian crayfish *Cherax tenuimanus* (Smith). *Comp. Biochem. Physiol.* A 95(1): 189–193.

Wheaton, F. W. 1977. *Aquacultural Engineering.* M. E. McCormick, ed. New York, N.Y.: John Wiley and Sons.

Wynn, T. M., and S. K. Liehr. 2001. Development of a constructed subsurface–flow wetland simulation model. *Ecol. Eng.* 16(4): 519–536.